

Whole-Body MRI and Whole Body [123I]-I-mIBG Scintigraphy: a Comparison in Intermediate and High Risk Neuroblastoma and validation of SIOPEN Scoring System in WB-MRI

Olianti C^{1*}, Perrone A², Allocca M³, Di Maurizio M², Carra F², La Cava G¹ and Tondo A²

¹University Hospital Careggi, Florence, Italy

²University Hospital A Meyer, Florence, Italy

³Hospital Brotzu-Cagliari, Italy

Abstract

Purpose: To assess the agreement between 123I-metaiodobenzylguanidine or [123I]-I-mIBG and Whole Body Magnetic Resonance Imaging with diffusion-weighted whole-body imaging with background body signal suppression (WB MRI-DWIBS) in High and Intermediate risk Neuroblastoma, a retrospective review was performed on [123I]-I-mIBG and DWIBS paired scans acquired at diagnosis, response-to-therapy, after-surgery, off therapy and after relapse with systemic involvement, and osteo-bone marrow metastatic load was evaluated for each of them.

Methods: 80 paired [123I]-I-mIBG and DWIBS scans were acquired for 31 patients between June 2009 and June 2019 within 30 days and without intercurrent therapy. SIOPEN Semi-quantitative Scoring Systems for NB with 12 body sections was applied at whole body MIBG and WB MRI-DWIBS acquired to evaluate the skeletal disease extent. In each case thoracic-abdominal SPECT was used to confirm or exclude doubtful scintigraphic alterations. We evaluated specificity, sensitivity, overall accuracy, positive predictive value (PPV) and negative predictive value (NPV) of WB MRI-DWIBS respect [123I]-I-mIBG scintigraphy considered as gold standard. The inverse theoretical statistic exercise was performed for [123I]-I-mIBG respect DWIBS results.

Results: DWIBS and [123I]-I-mIBG images were concordant in 890 out of the 960 analyzed segments, with high agreement between the two techniques (Kendal=0.85 $P < 0.0001$ and Chi 536.5975 $P < 0.0001$). Considering [123I]-I-mIBG as gold standard, WB MRI-DWIBS overall accuracy was 93%, sensitivity 78%, specificity 95%, PPV 77% and NPV 96%. Otherwise, on the theoretical statistic exercise, [123I]-I-mIBG overall accuracy was 93%; sensitivity 77%; specificity 97%; VPP 78%; VPN 95%, respect DWIBS. [123I]-I-mIBG and WB MRI-DWIBS SIOPEN scoring resulted superimposable (Rho Spearman=0.88, $P < 0.0001$).

Conclusion: DWIBS and [123I]-I-mIBG images showed a very high concordance: a first validation of SIOPEN Scoring System seems possible on the basis of these data. WB MRI may represent an alternative in weak-avid MIBG tumors and for follow up assessment. A multimodal imaging protocol is proposed for High and Intermediate Risk protocols.

Keywords: 123I-Metaiodobenzylguanidine • Scintigraphy • Scoring System • Whole Body Magnetic Resonance Imaging • Diffusion-Weighted Imaging • Neuroblastoma

Introduction

Neuroblastoma (NB) is the most frequent extracranial solid tumor of childhood, representing 8% to 10% of all cases of childhood cancer [1].

Overall survival for patients with low- and intermediate-risk neuroblastoma is excellent (greater than 90%), while overall survival for high-risk patients remains approximately 40%. Multimodality approaches have been developed to treat patients who are classified as high risk, whereas patients with low- or intermediate-risk neuroblastoma have received reduced therapy. This treatment approach has resulted in improved outcome, although survival for high-risk patients remains poor even if overall survival in neuroblastoma has improved [2,3].

Within the high risk neuroblastoma group the majority of patients (> 80%)

***Address for Correspondence:** Dr. Catia Olianti, University Hospital Careggi, Florence, Italy, E-mail: catia.olianti@unifi.it

Copyright: © 2021 Olianti C, et al. This is an open-access article distributed under the terms of the Creative Commons Attribution License, which permits unrestricted use, distribution, and reproduction in any medium, provided the original author and source are credited.

Received 28 June, 2021; Accepted 09 July 2021; Published 16 July 2021

have metastatic disease (stage IV) at the time of presentation and metastasis are most commonly present at cortical bone and bone marrow: at diagnosis is crucial the identification of metastatic sites to evaluate the metastatic load and the response to treatment [4].

The specificity of 123I-MetalodoBenzylGuanidine ([123I]-I-mIBG) for detecting primary and secondary neuroblastoma has always been estimated close to 100%, while the sensitivity is 90-95% [5]. More recently was found in neuroblastoma that [123I]-I-mIBG has a sensitivity of 88%-93% and a specificity of 83%-92% [6,7].

So, the guidelines recommend the use of Whole Body (WB) [123I]-I-mIBG scintigraphy to assess the extent of the disease and according to the International Neuroblastoma Risk Group Staging System (INRGSS) the scintigraphic uptake in the skeleton is a condition for considering a patient to be a metastatic stage M [8]. This is often true because soft-tissue distant metastasis, able to change diagnostic stage, is quite less frequent than skeletal metastasis.

Radioiodine-labeled MIBG is used to evaluate the metabolic MIBG-avidity of primary tumor and is the test of choice for identification of metastatic sites [9-11]. The addition of single photon emission computed tomography (SPECT) and SPECT/CT to [123I]-I-mIBG planar images have improved the identification and characterization of sites of uptake [12]. So guidelines on

molecular imaging in neuroblastoma recommend at the moment SPECT/CT as the state of the art molecular imaging technique in the upper part of body [13].

Nevertheless, [123I]-I-MIBG scintigraphy has some drawbacks as the radiation exposure, the weak or absent MIBG avidity in a 10% of neuroblastoma [5,6] and the suboptimal detection of small subcentimeter lesions [14,15]. Whole-body magnetic resonance imaging (WB MRI) has been used for evaluation of skeletal lesions, both for staging and follow-up in various oncologic diseases, without the exposure of the patient to ionizing radiation [16]. To our knowledge, few series have been published about the diagnostic performance of WB-MRI in patients with neuroblastoma compared to [123I]-I-MIBG scintigraphy [17,18]. In 2012, in a case report, Pai Panandiker et al. compared [123I]-I-MIBG scintigraphy with WB MRI with Diffusion-Weighted Imaging with background body signal Suppression (WB MRI-DWIBS) and proposed WB MRI for detecting small metastasis of neuroblastoma [19].

Recently, Ishiguchi et al. evaluated diagnostic performance of WB MRI-DWIBS and 18F-FDG PET/TC for detecting lymph node and bone metastasis in pediatric patients with neuroblastoma [20]. However, to date, no large series have been published in which the usefulness of WB MRI to assess the skeletal tumor burden of neuroblastoma in comparison with MIBG scintigraphy, considered as the reference standard, was evaluated.

Aim of this study is to assess the concordance between [123I]-I-MIBG WB scintigraphy and WB MRI with DWIBS for detecting bone metastasis in high and intermediate risk neuroblastoma (NB), in order to improve and integrate metabolic nuclear medicine data in almost all diagnostic-therapeutic steps of metastatic neuroblastoma protocols. A semi - quantitative scoring system for NB with 12 body sections was applied at whole body [123I]-I-MIBG and WB MRI-DWIBS acquired to evaluate the skeletal disease extent.

Materials and Methods

Patients' population

We retrospectively evaluated 31 consecutive patients (mean age: 6.46 ± 12.05 years; range 3 months -16 years and 4 months; 21 males, 10 females) with high risk-NB (19 HR-NB, 61%) and intermediate risk NB (12 L2-NB, 39%); four patients had relapse with metastatic skeletal involvement after completed standard diagnostic-therapeutic Lines protocol.

A total amount of 82 paired whole body and SPECT MIBG and WB-MRI/DWIBS scans were acquired between June 2009 and June 2019 within 30 days, without intercurrent therapy. Two couple WB MIBG scintigraphy and WB MRI-DWIBS were rejected because of intercurrent chemo-therapy (CH); therefore, our data set included 80 paired WB [123I]-I-MIBG scintigraphy-WB MRI-DWIBS. Two expert Nuclear Medicine Physicians (more than 10-20 year of activity) and two expert Radiologists (more than 8-10 years of activity) performed the readings of WB-scans on the basis of International Society of Pediatric Oncology Europe Neuroblastoma SIOOPEN scoring system.

This retrospective study had institutional review board approval; written informed consent was obtained from all Parents or Guardians.

Whole-Body 123I-MIBG scintigraphy

All diagnostic 123I-MIBG scans were performed on the basis of 2002-2018 guidelines for scintigraphic examinations of NB [13,14,21]. Each patient received a 123I-MIBG dose activity in accordance with European Association of Nuclear Medicine (EANM) dosage calculator, 5.18 MBq/kg was administered, with a maximum dose of 185 MBq (most of patients had a weight under 25Kg, one has a weight of 38Kg with a maximum activity administered 236 MBq) [20,21]. All of them underwent to thyroid tissue iodine prophylaxis with Lugol's solution 5%, range 8-40 drops on the basis of weigh and age [21]. Whole Body vertex-feet and SPECT thoracic-abdominal tract images were acquired at about 24 hours, the first performed with 5-7 cm/min. bed velocity or 400 Kcounts for each spot scans 128 × 128 matrix; the second with shoot and stop 3degrees projections 20-30 sec./step, according to EANM GL 2010, 20 patients on a Picker Philips Medical System and 11 patients more recently on a SIEMENS ECAM Gamma-camera, both equipped with MEGP parallel hole collimator [22].

All scintigraphic scans were acquired after voiding and for younger than three years children after voiding and diaper change. No patient needed a catheterization, only one had a catheter for clinical reasons. No patients underwent sedo-analgesia procedure; in last two years some of younger and less compliant patients had premedication with 1-3 mg of melatonin per os one hour before scan to induce a transient para-physiological sleep or a more relaxed state. Melatonin was useful in our own experience but a wider feasibility should be yet assessed. Most of the other children performed scans asleep at the presence of parents with entertainment methods (tablet with cartoons or baby-songs).

SIOOPEN Scoring System

According to the SIOOPEN semiquantitative scoring method, the skeleton was divided into 12 anatomical body segments as follows: the skull, the thoracic cage, the proximal right upper limb, the distal right upper limb, the proximal left upper limb, the distal left upper limb, the spine, the pelvis, the proximal right lower limb, the distal right lower limb, the proximal left lower limb and the distal left lower limb. The extent and pattern of skeletal MIBG involvement was scored using a 0-6 scale to discriminate between focal discrete lesions and patterns of more diffuse infiltration [22-24]. As known this method define lesion extension with a 0-6 grade scoring: 0 no sites per segment, 1 one discrete site per segment, 2 two discrete sites per segment, 3 three discrete lesions, 4 more than three discrete foci or a single diffuse lesion involving <50% of the segment, 5 diffuse involvement of 50-95% of the segment, and 6 diffuse involvement of the entire segment (Figure 1, and Table 1) [24]. SPECT acquisition is usually useful in evaluation of difficult to read body segments i.e. neck, abdomen and spine for physiological superimposing images (salivary glands, activated brown fat, intestinal and bladder content, hepatic or spleen physiological activity close to adrenals) [5]. So, this scan, always performed in thoracic-abdomen district, was used to confirm [123I]-I-MIBG-WB metabolic alterations and for controversial founding. Curie Scoring System which includes primary tumor and soft tissue involvement wasn't applied to our population cause we wanted evaluate only skeletal tumor burden as considered in SIOOPEN Scoring System [24]. Moreover we found very few soft tissue not-primary tumor localizations in our series.

Whole body MRI with diffusion-weighted imaging with background body signal suppression (WB MRI-DWIBS)

MR examination was performed using a 1.5 or 3T scanner (Achieva and Achieva D-Stream, respectively; Philips Medical Systems, The Netherland) with patient in supine feet-first position; 58 exams were performed on 1.5T scanner and 22 exams on 3T equipment. Whole-body images were obtained with three or more consecutive package acquisitions, depending on body height, using Q-body coil for signal receiving and transmitting. The imaging protocol consisted of a coronal T2-weighted short time inversion-recovery (T2W-STIR) and of an axial diffusion weighted imaging with background body signal suppression (DWIBS) sequence. DWIBS was acquired using a short TI inversion recovery echo-planar imaging (STIR-EPI) sequence under free breathing applying one b-value (800 and 1000 s/mm² respectively for 3T and 1,5T scanner) in 62 exams and four b-value (0, 100, 200 and 800 s/mm²) in 18

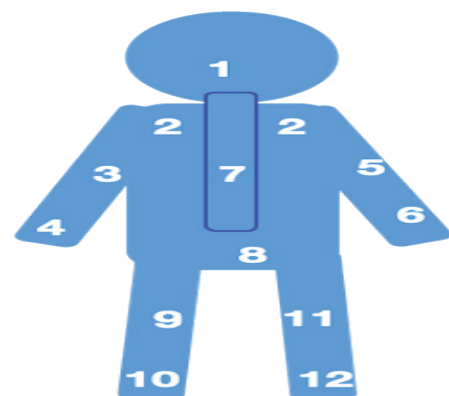


Figure 1. Numbering of 12 segments.

Table 1. SIOPEN Scoring System : 12 segments, 6 grades.

S. No	12 Segments	Pattern of Scheletal Involvement, 6 Grades
1	Head	0 no lesions
2	Thorax	1 one lesion
3	Right Humerus	2 two lesions
4	Right Forearm	3 three lesions
5	Left Humerus	4 > 3 lesions < 50% of segment
6	Left Forearm	5 > 50% < 90% of segment
7	Spine	6 > 90% of segment
8	Pelvis	
9	Right Femur	
10	Right Tibia	
11	Left Femur	
12	Left Tibia	

cases performed on 3T scanner.

Multiplanar reconstructions (MPR) images and high-resolution maximum intensity projection (MIP) images were reconstructed in all cases.

Total acquisition time for whole-body MRI was approximately 45-50 minutes. Younger or uncooperative children underwent general inhalation anesthesia with maintenance of spontaneous breathing and monitoring of vital parameters (heart rate, respiratory rate, SpO₂, EtCO₂), during performing MR examinations, in the presence of the anesthetist.

WB MRI Image Analysis

Whole-body MRI data sets were transferred to a Picture Archiving and Communications System (PACS). Two independent radiologists with 10 and 8 years of WB MRI experience, respectively, blinded to 123I-MIBG scintigraphy, evaluated in consensus MR images. On MR images bone marrow involvement was considered positive if present abnormal and/or focal increase of DWIBS and/or STIR intensity not from normal anatomic structure; DWIBS was evaluated only visually, in comparison with signal intensity of skeletal muscle. Quantitative analysis of ADC value (ADC, apparent diffusion coefficient) was not performed in this study. In case of discrepancies between STIR and DWIBS images, we considered as "true" DWIBS results. SIOPEN scoring System was also applied to all WB MRI-DWIBS scans using the same scintigraphic criteria.

Statistical Analysis

Specificity, sensitivity, overall accuracy, VPP and VPN of WB MRI were estimated respect MIBG considered as gold standard. We performed furthermore the same analysis taking WB MRI-DWIBS as gold standard. As theoretical statistical exercise, we evaluate the overall accuracy for [123I]-MIBG vs DWIBS results, even if MIBG remains at the moment the real gold standard. Chi-square, parametric and not-parametric correlations were used to assess agreement degree among total scoring value, number of lesions, mean of scoring for each segment. T di Student for coupled data and mean comparison were used to compare mean±SD and % of segments resulted site of lesions among 80 paired data. $p < 0.05$ is considered as significative. Comparison between means for scoring data in pathological segments was studied with the Kendal-coefficient concordance and the sign-test. Wilcoxon test was used to compare the % of segments resulted as pathological.

The few number of patients and the inhomogeneous entity of groups in different steps of HR and Lines protocols didn't allow a statistical evaluation of SIOPEN Score results in each single steps of pathway: diagnosis, after induction-CHT, after Surgery, before High-Dose CHT, after Radiotherapy. We would perform this evaluation in larger series.

Results

Our series enclosed 27/31Patients at staging (87%), 17/31 after induction-CH (55%), 14/31 after relapse (45%). Stage-related comparison about SIOPEN score value and number of alterations was performed in WB-MIBG

and WB-DWIBS : at staging not significant differences was found in total SIOPEN scoring values (3.5 ± 8.8 MIBG vs 5.33 ± 11.1 DWIBS mean \pm SD; $p=0.53$) and for number of alterations (5 ± 13.7 MIBG vs 7.33 ± 16.5 DWIBS mean \pm SD; $p=0.6$). After induction-CHT not significant differences existed in total SIOPEN scoring values (1.71 ± 4.7 MIBG vs 3.12 ± 6.28 DWIBS mean \pm SD; $p=0.46$) and for number of alterations (1.71 ± 4.7 MIBG vs 3.5 ± 7.13 DWIBS mean \pm SD; $p=0.43$). At relapse not significant differences existed in total SIOPEN scoring values (1.29 ± 2.94 MIBG vs 1.43 ± 2.29 DWIBS mean \pm SD; $p=0.89$) and for number of alterations (1.36 ± 2.4 MIBG vs 1.43 ± 2.93 DWIBS mean \pm SD; $p=0.95$).

In whole population WB MRI-DWIBS and MIBG scoring evaluations were concordant in 890 out of the 960 analyzed segments: 769 negative concordant sites (80.1%), 121 positive concordant (12.6%); 36 DWIBS positive but MIBG negative sites (3.7%), 34 DWIBS negative but MIBG positive sites (3.5%), with high agreement between the two diagnostic techniques ($\kappa=0.85$, $P < 0.0001$ and Chi-square statistic 536.5975, $P < 0.00001$). Example of concordant sites is shown in Figure 2. Images of discordant cases with false-positive WB-MRI are shown in Figure 3, while false-negative MIBG scintigraphy images in one case of weak avid neuroblastoma at onset is shown in Figure 4. We report another discordant case with weak inhomogeneous MIBG uptake in thoracic primary tumor and a focal intense alteration on dorsal spine, not clearly visible detected at DWIBS images (Figure 5).

Considering MIBG as gold standard, WB MRI-DWIBS overall accuracy was 93%, sensitivity 78%, specificity 95%, PPV 77% and NPV 96%. Otherwise, if we consider WB MRI-DWIBS as gold standard, MIBG overall accuracy was 93%, sensitivity 77%, specificity 97%, PPV 78% and NPV 95%. Thus, MIBG and WB MRI SIOPEN scoring resulted superimposable (Rho Spearman=0.88, $P < 0.0001$) (Table 2).

Mean scoring value for MIBG and DWIBS in whole cohort of patients was 4.54 ± 12 mean \pm SD for MIBG and 4.64 ± 9 mean \pm SD for WB MRI DWIBS, with median value 0 (51%) and range 0-45 and median value 0 (57%) and range 0-42 respectively; considering only the pathologic segments we found 9.31 ± 12 mean \pm SD for MIBG and 10.91 ± 12 mean \pm SD for WB MRI-DWIBS with a median value 4 and range 1-45 and median value 6 and range 1-42 respectively (Table 3).

If we consider the total number of lesions for MIBG and WB MRI-DWIBS we found in the whole cohort of patients the mean value of 5.25 ± 9 mean \pm SD for MIBG and 5.49 ± 12 mean \pm SD for WB-MRI/DWIBS, with median value 0 (51%) and range 0-56 and median value 0 (57%) and range 0-60 respectively; if we consider only the pathologic segments we found 10.8 ± 16 mean \pm SD for MIBG and 12.91 ± 16 mean \pm SD for WB-MRI with a median value 3 and range 1-56 and median value 5 and range 1-60 respectively (Table 3).

Both parametric and not-parametric tests for paired data showed a very good concordance between MIBG and DWIBS: for mean scoring values were

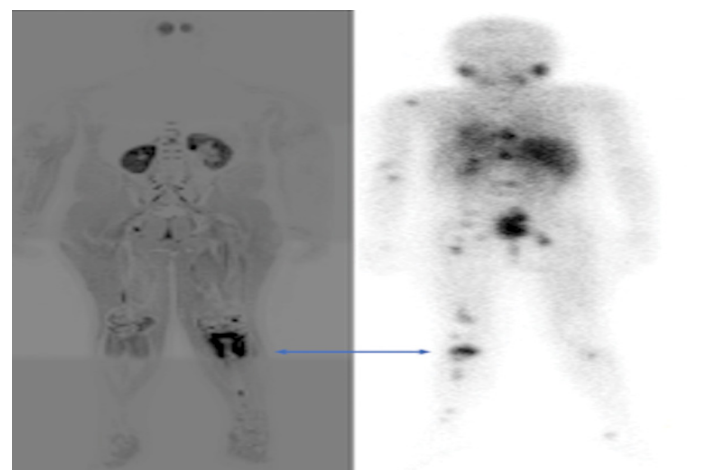


Figure 2. Left knee intense DWIBS –WB restriction diffusion alteration and skeletal intense MIBG uptake in HR-NB, arrow.

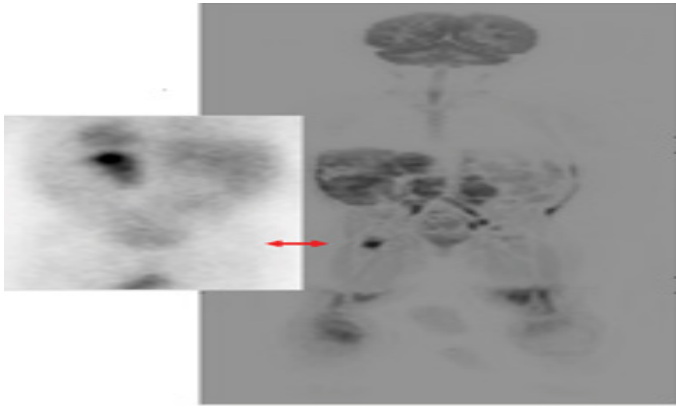


Figure 3. False positive DWIBS –WB on right proximal femur versus a negative MIBG scan, arrow.

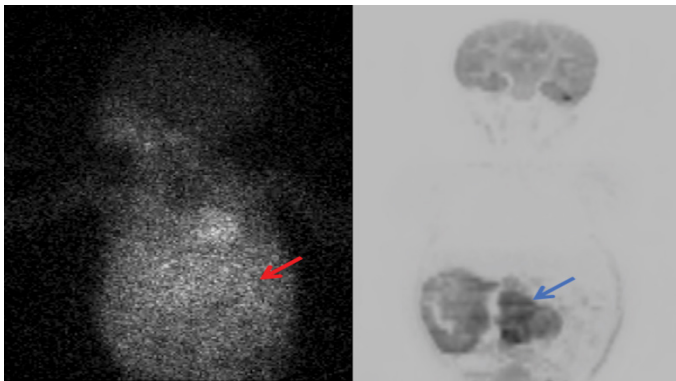


Figure 4. High DWIBS – WB restricted diffusion on a large abdominal primary tumor with a few-avid MIBG abdominal uptake in a Lines NB at staging.

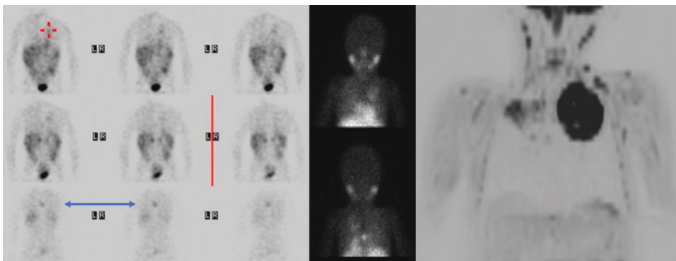


Figure 5. Large intense DWIBS –WB diffusion-restricted area on left thorax versus a mild visualization on MIBG scan, where instead is well evidenced an intense MIBG spine alteration (spinous process) arrow. Revision of whole tumor histopathology showed a small site of NB in a big thoracic ganglioneuroblastoma with supraclavicular benign lymphonodes.

found a Pearson correlation R value of 0.81 and a Rho Spearman value of 0.97, $p < 0.0001$; for total number of lesions in whole population R 0.78 and Rho 0.97, $p < 0.0001$; only in pathologic segments, mean scoring value correlation had R 0.82 and Rho 0.97, $p < 0.0001$, and R 0.78 and Rho 0.96, $p < 0.0001$ for total number of lesions [Table 4].

The comparison of paired data mean-scoring per-segment and % of segments, resulted site of disease, didn't show any significant difference: $t=0.62$ with $p=0.54$ for mean-scoring and $t=0.46$ with $p=0.65$ for % of pathologic segments. Non-parametric test, (Kendal-coefficient concordance) $K= 0.76$; sign-test =1. Wilcoxon test for % of pathologic segments $p=0.61$ and for mean-scoring $p=0.66$.

Metastatic lymphadenopathy and soft tissue involvement was very infrequent in our series, and their presence was mostly irrelevant for stage evaluation cause always loco-regional. Only one Patient had liver metastasis, only one neoplastic vein caval thrombosis and only two had pulmonary metastasis on end stage of disease. None brain metastasis was found in our series [25,26].

Table 2. Accuracy, sensitivity, specificity, positive predicting value PPV, negative predicting value NPV for MIBG and DWIBS considered as gold-standard each other.

	True Positive MIBG	True Negative MIBG	Total		
DWIBS +	121 (12.6%)	36 (3.7%)	157	78%	VPP
DWIBS -	34 (3.5%)	769 (80.1%)	803	95%	VNN
Total	155	805	960		
	78%	93%	92%		Chi-Square 440
	Sensitivity	Specificity	Accuracy		$P < 0.0001$

	True Positive DWIBS	True Positive DWIBS	Total		
MIBG +	121 (12.6%)	34 (3.5%)	155	78%	VPP
MIBG -	36 (3.6%)	769 (80.1%)	805	96%	VPN
Total	157	803	960		
	77%	96%	93%		Chi-Square 435
	Sensitivity	Specificity	Accuracy		$P < 0.0001$

Table 3. Mean \pm SD MIBG and DWIBS scoring and total number of lesions (Rho Spearman and Pearson correlation, significance) on whole 80 paired data sets A, and only on pathologic segments for MIBG and DWIBS B.

	All segments A	MIBG	DWIBS	Rho Spearman	Pearson
Total scoring mean \pm SD		4.54 \pm 12	4.64 \pm 12	0.81	0.97
				$P < 0.0001$	$P < 0.0001$
Median		0 (51%)	0 (57%)		
Range		0-45	0-45		
Total number of lesions mean \pm SD		5.25 \pm 9	5.49 \pm 12	0.82	0.97
				$P < 0.0001$	$P < 0.0001$
Median		0 (51%)	0 (57%)		
Range		0-56	0-60		
Positive segments B					
Total scoring mean \pm SD		9.31 \pm 12	10.91 \pm 12	0.78	0.96
				$P < 0.0001$	$P < 0.0001$
Median		4	6		
Range		1-45	1-42		
Total number of lesions mean \pm SD		10.8 \pm 16	12.91 \pm 16	0.72	0.96
				$P < 0.0001$	$P < 0.0001$
Median		3	5		
Range		1-56	1-60		

Discussion

A feasible conclusion from the results presented is that, in this series of patients with neuroblastoma, MRI showed a good concordance with regard to bone-marrow metastatic lesions, and that these results allow a first-step validation of the use of SIOPEN Scoring System and counting of number of alterations in Whole Body DWIBS-MRI.

MRI is an effective method for imaging neuroblastoma [27]. It shows high sensitivity in detecting bone marrow metastases, high intrinsic soft tissue contrast resolution, precise definition of intraspinal tumor extension, good delineation of diaphragmatic involvement of thoracic tumors [28]. WB MRI may represent a radiation-free alternative in the assessment of patients with NB and its feasibility has already been demonstrated for the work-up of oncologic patients with various neoplastic diseases, (e.g., melanoma, breast, colorectal, prostate cancers) or for hematologic diseases with nodal or bone marrow involvement (lymphoma, multiple myeloma) [29,30].

WB MRI uses both conventional sequences which provide predominantly anatomical information; such STIR e T1 weighted sequences, and functional

Table 4. Mean \pm SD MIBG and DWIBS scoring in each segment (Rho Spearman correlation, significance) on only pathologic segments for MIBG and DWIBS.

S. No	Segments	MIBG	%	DWIBS	%	Rho Spearman	Sig.	mean	%
1	Head	2.2 \pm 1.5	21	1.9 \pm 1.3	19	0.64	$P < 0.0001$	> M	> M
2	Thorax	2.4 \pm 1.6	17	1.9 \pm 1.4	20	0.93	$P < 0.0001$	> M	> D
3	Right Humerus	3.4 \pm 1.8	19	2.3 \pm 1.3	16	0.91	$P < 0.0001$	> M	> M
4	Right Forearm	1.9 \pm 0.9	20	2 \pm 1.1	17.5	0.87	$P < 0.0001$	> D	> M
5	Left Humerus	1 \pm 0	2.5	1.3 \pm 1.6	3.7	0.38	$P < 0.0001$	> D	> D
6	Left Forearm	1.4 \pm 0.5	6	1.6 \pm 0.5	6	0.79	$P < 0.0001$	> D	—
7	Spine	2.9 \pm 2	25	3.14 \pm 1.6	26	0.73	$P < 0.0001$	> D	> D
8	Pelvis	4 \pm 1.2	15	3.6 \pm 1.6	22.5	0.76	$P < 0.0001$	> M	> D
9	Right Femur	2.1 \pm 1.3	22.5	1.9 \pm 1.2	22.5	0.78	$P < 0.0001$	> M	—
10	Right Tibia	2.3 \pm 1.4	19	2.3 \pm 1.4	21	0.68	$P < 0.0001$	—	> D
11	Left Femur	1.8 \pm 1.2	12.5	2 \pm 0.9	10	0.77	$P < 0.0001$	> D	> M
12	Left Tibia	2.2 \pm 1.6	14	2.7 \pm 1.8	11	0.71	$P < 0.0001$	> D	> M

sequences, such DWI and/or DWIBS. As known, DWIBS is a particular DWI technique that provides functional information from entire body during free breathing, in high signal-to-noise ratio (SNR) images, leading to easy identification of small lesions and thereby helping to visualize the spread of the disease [31].

In particular, as regards neuroblastic tumors, DWI sequence, based on ADC maps, has been shown to be able to distinguish between benign and malignant neuroblastic tumors, and to be useful in evaluating the response to chemotherapy [32-35].

In the present study, we evaluated the diagnostic accuracy of WB MRI-DWIBS in the assessment of the burden of disease, compared to MIBG WB Scintigraphy considered as gold standard, applying SIOPEN scoring system to both methods. The SIOPEN scoring systems have been used in large international clinical trials, showing to provide important prognostic information that can be used to guide appropriate therapy [36].

Our study demonstrates a good concordance about diagnosis, response to therapy and relapse evaluation scored by SIOPEN system on MIBG WB Scintigraphy and WB MRI-DWIBS. The two diagnostic techniques showed a high agreement of 92.7% of segments evaluated (80.1% negative concordant sites and 12.6% positive concordant sites) and resulted discordant in only 7.2% of segments evaluated (3.5% DWIBS negative but MIBG positive sites and 3.7% DWIBS positive but MIBG negative sites). Both mean scoring values for positive segments and percentage of segments appear superimposable, with few light differences of performance and high Rho Spearman value. The scoring evaluation shows in our court of segments about a 20% of metastatic involvement in bone marrow for skull, thorax, spine, pelvis, femur and tibia, less percentage for the other sites.

Most of few discordant results regards skull, thorax and pelvis (slightly more sensitivity of MIBG), spine and limbs (slightly more sensitivity of MRI). As for ribs and skull, the lower sensitivity of WB MRI might be explained by thin thickness of these bones; to overcome the weakness on this segment we could perform as additional sequence an axial STIR sequence with thin thickness.

WB MIBG and WB MRI had high statistically significant agreement. Thus considering MIBG as gold standard, WB-MRI overall accuracy is 93%, sensibility 78%, specificity 95%, VPP 77% and VPN 96%. MIBG and WB-MRI SIOPEN scoring resulted superimposable (Rho Spearman=0.88, $P < 0.0001$) with a light prevalence for MRI for sensitivity and a light prevalence for MIBG about specificity as well known in clinical practice.

Also, the mean value of scoring for each segment shows a light prevalence of WB MRI on WB MIBG because of the higher sensitivity on smaller signal-alterations related to the different resolution of two diagnostic method: about 7 -10 mm for MIBG and about 4 mm for MRI [25,30]. Our data confirm also the assessment that MIBG scintigraphy is the best established and most widely used scintigraphic technique in the evaluation of NB because of its high sensitivity (97%) and specificity (83%-92%) [28]. A combination of MRI and MIBG scintigraphy has been shown to achieve the best sensitivity and specificity in NB imaging [21]. In our series this was quite true for the very few number of soft tissue metastasis at staging and at relapse.

Scintigraphy exposes patients to ionizing radiation. This is a major concern in children, who are at higher risk because of their smaller body size, higher mitotic rate, and longer life expectancy, in particular for low and intermediate risk NB [37].

According to protocol HR-NB, at least 7 MIBG- scintigraphy are necessary during the different steps of therapy with a high number of diagnostic examinations, and increased risk of potential secondary malignancies [13,37]. Leverdiere et al. found that the cumulative incidence of second malignant neoplasms in long survivor of neuroblastoma was 3.5% at 25 years and 7.0% at 30 years after diagnosis. Compared with the sibling cohort, survivors had an increased risk of selected chronic health conditions (risk ratio [RR]=8.3; 95% CI=7.1 to 9.7) with a 20-year cumulative incidence of 41.1%. Endocrine complications are prevalent in childhood cancer survivors, with 50% experiencing at least one hormonal disorder over the course of their lives [38,39]. Moreover, Mostoufi et al. demonstrated at least one (16.7%) at least two (8.6%) and three or more (6.6%) endocrinopathies in survivors of neuroblastoma (31.9%) [40].

At our knowledge no other published study exists designed to perform a systematic comparison of SIOPEN Scoring on WB MIBG scintigraphy and on WB MRI-DWIBS. This may represent an important innovation about diagnostic evaluation and semi-quantitative scoring of HR-NB and Intermediate-Risk NB. In our experience, the clinical introduction of WB MRI may be useful in diagnostic protocol of NB with very high accuracy in disease extension and functional complemental characterization of primary tumor and bone-marrow-metastasis. Further studies, also with Curie Score evaluation, are necessary to check soft tissue involvement. This is even more important for those cases with weak or poor MIBG avidity, due to the degree of undifferentiation of tumor cells, as well as for neuroblastoma with loss of MIBG avidity at relapse, as demonstrated in two cases of our series [17]. Also, in our experience, a combination of MRI and MIBG scintigraphy showed to achieve the best sensitivity and specificity in NB imaging.

As known, a limitation of WB MRI is the light overestimation of bone lesions, especially in post-chemotherapy examinations. At the onset, the false-positive findings at DWIBS sequences are often due to the high signal of the regions rich in red bone marrow in the normal developing skeleton, above all in lumbar spine and pelvic skeleton as reported by Muller et al. [41]. Therefore, the radiologist experience is fundamental in the identification of these areas of physiological hyper-intensity.

WB MRI shows lightly less specificity compared to MIBG scintigraphy also during the evaluation of therapy response as it arises from our results, whose statistical analysis seems assess a fine concordance between MIBG and DWIBS, with a bit greater scoring value and number of alterations respect MIBG. This limit of DWIBS sequence can be explained in part by the so-called "T2 shine-through" phenomenon: high signal on diffusion-weighted images is not due to restricted diffusion, but rather to high T2 signal which 'shines through' to the DWI image. It can be overcome by evaluating the apparent diffusion coefficient (ADC), a value that measures the effect of diffusion independent of

the influence of T2 shine-through, but our study lacks a quantitative analysis [42]. Nevertheless, there are no validated bone ADC criteria in the literature, and there is a poor reproducibility of ADC measurements especially if the regions examined are "small". Furthermore, it should be added that especially in the evaluation of bone marrow there is a need to consider how the different types of treatment (chemotherapy, radiotherapy, immunotherapy) can affect the modification of the bone marrow signal intensity, data to date not yet clearly known [43,44]. These could be other interesting items for further studies. An important limitation is given by the lack of a standardized technique in the execution of the WB MRI, with different protocols among the numerous published studies. Another weakness is the non-capillary diffusion of MRI instrumentation. Finally, the necessity of general inhalation anesthesia for less than four years old patients or for not collaborative ones, with the assistance of the pediatric anesthetist might be another limitation of MRI application. This is otherwise true also for scintigraphic acquisitions in particular for SPECT-CT modality.

Conclusion

WB MRI-DWIBS and WB MIBG scintigraphy can be considered as complementary tools in the evaluation of metastatic NB at the diagnosis and during the evaluated steps of protocols. We propose an integrated diagnostic model where WB MRI-DWIBS could avoid the necessity or MIBG scan in some of multiple steps of HR and reduce thus the number of diagnostic MIBG scans in the course of HR and low and intermediate risk NB protocol. We usually perform both exams at staging, post-induction, post-surgery, before maintenance and at the end of treatment especially when not-primary tumor soft tissue involvement is absent; in the steps post-high dose chemotherapy MIBG could be omitted in case of stable negativity of WB MRI-DWIBS. WB MRI assessment could be useful without any other diagnostic modality during the follow up: 123I-MIBG scan should be performed to confirm or exclude relapse, for the eventual re-staging, and for metabolic typification of skeletal or soft tissue new lesions. Another possible employment of WB MRI imaging is relative to children with instable systemic onset of neuroblastoma, who need a staging assessment into a short time interval; WB MRI could allow both an evaluation of primary tumor with focused sequences and an evaluation of skeletal and extra-skeletal metastases, in a single exam without radiation exposure. Thus, as already affirmed a good combination of MRI and MIBG scintigraphy allows achieving the best sensitivity and specificity in NB imaging.

Acknowledgments

This work is written in memory of Dott. Claudio Defilippi pediatric radiologist, our mentor and friend. The Authors thank a lot Dott. Claudio Favre.

Authors' Contribution Statements

Conceptualization: (Annalisa Tondo), Methodology: (Catia Olianti); Formal analysis and investigation: (Catia Olianti, Michela Allocca, Anna Perrone, Marco Di Maurizio); Writing - original draft preparation: (Catia Olianti, Anna Perrone); Writing - review and editing-Supervision: (Annalisa Tondo, Federica Carra), Supervision: (Giuseppe La Cava)

Availability of Data and Materials

The authors give their availability to any queries.

Ethics Approval

All procedures performed in studies involving human participants were in accordance with the ethical standards of the institutional and/or national research committee and with the 1964 Helsinki declaration and its later amendments or comparable ethical standards.

Conflict of Interest

Author Catia Olianti declares that she has no conflict of interest. Author Anna Perrone declares that she has no conflict of interest. Author Michela Allocca declares that she has no conflict of interest. Author Marco Di Maurizio declares that he has no conflict of interest. Author Federica Carra declares that she has no conflict of interest. Author Giuseppe La Cava declares that he has no conflict of interest. Author Annalisa Tondo declares that she has no conflict of interest.

Informed Consent

Informed consent was obtained from all individual participants included in the study.

Funding

This study wasn't funded.

References

- Park, Julie R, Angelika Eggert and Huib Caron. "Neuroblastoma: Biology, Prognosis and Treatment." *Hematol Oncol Clin North Am* 24(2010): 65-86.
- Wilson, LM Kinnier and GJ Draper. "Neuroblastoma, its Natural History and Prognosis: A Study of 487 Cases." *Br Med J* 3(1974): 301-307.
- Pinto, Navin R, Mark A Applebaum, Samuel L Volchenboum and Katherine K Matthay, et al. "Advances in Risk Classification and Treatment Strategies for Neuroblastoma." *J Clin Oncol* 33(2015): 3008.
- Naranjo, Arlene, Meredith S Irwin, Michael D Hogarty and Susan L Cohn, et al. "Statistical Framework in Support of a Revised Children's Oncology Group Neuroblastoma Risk Classification System." *JCO Clin Cancer Inform* 2(2018): 1-15.
- Jacobs, Aurélie, M Delree, B Desprechins and Jacques Otten, et al. "Consolidating the Role of I-MIBG-Scintigraphy in Childhood Neuroblastoma: Five Years of Clinical Experience." *Pediatr Radiol* 20(1990): 157-159.
- Vik, Terry A, Thomas Pfluger, Richard Kadota and Victoria Castel, et al. "123I Mibg Scintigraphy In Patients With Known Or Suspected Neuroblastoma: Results from a Prospective Multicenter Trial." *Pediatr Blood Cancer* 52(2009): 784-790.
- Liu, B, H Zhuang and S Servaes. "Comparison of [123I] MIBG and [131I] MIBG for Imaging of Neuroblastoma and other Neural Crest Tumors." *Q J Nucl Med Mol Imaging* 57(2013): 21-28.
- Monclair, Tom, Garrett M Brodeur, Peter F Ambros and Hervé J Brisse, et al. "The International Neuroblastoma Risk Group (INRG) Staging System: An INRG Task Force Report." *J Clin Oncol* 27(2009): 298.
- Brodeur, Garrett M, Jon Pritchard, Frank Berthold and NL Carlsen, et al. "Revisions of the International Criteria for Neuroblastoma Diagnosis, Staging and Response to Treatment." *J Clin Oncol* 11(1993): 1466-1477.
- Sharp, Susan E, Andrew T Trout, Brian D Weiss and Michael J Gelfand. "MIBG in Neuroblastoma Diagnostic Imaging and Therapy." *Radiographics* 36(2016): 258-278.
- Brisse, Hervé J, M Beth Mccarville, Claudio Granata and K Barbara Krug, et al. "Guidelines for Imaging and Staging of Neuroblastic Tumors: Consensus Report from the International Neuroblastoma Risk Group Project." *Radiol* 261(2011): 243-257.
- Matthay, KK, B Shulkin, R Ladenstein and J Michon, et al. "Criteria for Evaluation of Disease Extent by 123 I-Metaiodobenzylguanidine Scans in Neuroblastoma: A Report for the International Neuroblastoma Risk Group (INRG) Task Force." *Br J Cancer* 102(2010): 1319-1326.
- Olivier, Pierre, Paula Colarinha, Jure Fettich and Sibylle Fischer, et al. "Guidelines for Radioiodinated MIBG Scintigraphy in Children." *Eur J Nucl Med Mol Imaging* 30(2003): B45-B50.
- Bombardieri, Emilio, Francesco Giammarile, Cumali Aktolun and Richard P Baum,

- et al. "131 I/123 I-Metaiodobenzylguanidine (Mibg) Scintigraphy: Procedure Guidelines for Tumour Imaging." *Eur J Nucl Med Mol Imaging* 37(2010): 2436-2446.
15. Yanik, Gregory A, Marguerite T Parisi, Barry L Shulkin and Arlene Naranjo, et al. "Semi-quantitative Mibg Scoring as a Prognostic Indicator in Patients with Stage 4 Neuroblastoma: A Report from the Children's Oncology Group." *J Nucl Med* 54(2013): 541-548.
 16. Kwee, Thomas C, Taro Takahara, Malou A Vermoolen and Marc B Bierings, et al. "Whole-Body Diffusion-Weighted Imaging for Staging Malignant Lymphoma in Children." *Pediatr Radiol* 40(2010): 1592-1602.
 17. Goo, Hyun Woo. "Whole-Body MRI of Neuroblastoma." *Eur J Radiol* 75(2010): 306-314.
 18. Goo, Hyun Woo, Seong Hoon Choi, Thad Ghim and Hyung Nam Moon, et al. "Whole-Body MRI of Paediatric Malignant Tumours: Comparison with Conventional Oncological Imaging Methods." *Pediatr Radiol* 35(2005): 766-773.
 19. Panandiker, Atmaram S Pai, Jamie Coleman and Barry Shulkin. "Whole Body Pediatric Neuroblastoma Imaging: 123I-Mibg and Beyond." *Clin Nucl Med* 40(2015): 737.
 20. Ishiguchi H, Ito S, Kato K. Diagnostic Performance of 18F-FDG PET/CT and Whole-Body Diffusion-Weighted Imaging with Background Body Suppression (DWBS) in Detection of Lymph Node And Bone Metastases from Pediatric Neuroblastoma. *Ann Nucl Med* 32: 348-362.
 21. Bar-Sever Z, Biassoni L and Shulkin B. Guidelines on Nuclear Medicine Imaging in Neuroblastoma. *Eur J Nucl Med Mol Imaging* 11(2018): 2009-2024.
 22. Lassmann, Michael and S Ted Treves. "Pediatric Radiopharmaceutical Administration: Harmonization of the 2007 EANM Paediatric Dosage Card (Version 1.5. 2008) and the 2010 North American Consensus Guideline." *Eur J Nucl Med Mol Imaging* 41(2014): 1636-1636.
 23. Matthay, KK, B Shulkin, R Ladenstein and J Michon, et al. "Criteria for Evaluation of Disease Extent by 123 I-Metaiodobenzylguanidine Scans in Neuroblastoma: A Report for the International Neuroblastoma Risk Group (INRG) Task Force." *Br J Cancer* 102(2010): 1319-1326.
 24. Decarolis, Boris, Christina Schneider, Barbara Hero and Thorsten Simon, et al. "Iodine-123 Metaiodobenzylguanidine Scintigraphy Scoring Allows Prediction of Outcome in Patients with Stage 4 Neuroblastoma: Results of the Cologne Interscore Comparison Study." *J Clin Oncol* 31(2013): 944-951.
 25. Sharp, Susan E, Barry L Shulkin, Michael J Gelfand and Shelia Salisbury, et al. "123I-MIBG Scintigraphy and 18F-FDG PET in Neuroblastoma." *J Nucl Med* 50(2009): 1237-1243.
 26. Orr, Katharine E and Kieran Mchugh. "The New International Neuroblastoma Response Criteria." *Pediatr Radiol* 49(2019): 1433-1440.
 27. Siegel, Marilyn J and Alok Jaju. "MR Imaging of Neuroblastic Masses." *Magn Reson Imaging Clin N Am* 16(2008): 499-513.
 28. Ladenstein, Ruth, Ulrike Pötschger, Dominique Valteau-Couanet and Roberto Luksch, et al. "Investigation of the Role of Dinutuximab Beta-Based Immunotherapy in the SIOPEN High-Risk Neuroblastoma 1 Trial (HR-NBL1)." *Cancers* 12(2020): 309.
 29. Wang, Xinzeng, Ali Pirasteh, James Brugarolas and Neil M Rofsky, et al. "Whole Body MRI for Metastatic Cancer Detection Using T2-Weighted Imaging with Fat and Fluid Suppression." *Magn Reson Med* 80(2018): 1402-1415.
 30. Bohlscheid, A, D Nuss, S Lieser and HP Busch. "Tumor Search with Diffusion-Weighted Imaging. First Experiences; Tumorsuche Mittels Kernspintomografischer Diffusionsbildgebung. Erste Erfahrungen." *Roefo-Fortschritte Auf Dem Gebiete Der Roentgenstrahlen Und Der Neuen Bildgebenden Verfahren* 180(2008): 302-309.
 31. Takahara T, Imai Y, Yamashita T and Yasuda S, et al. Diffusion Weighted Whole Body Imaging With Background Body Signal Suppression (DWBS): Technical Improvement Using Free Breathing, STIR And High Resolution 3D Display. *Radiat Med* 22(2004): 275-282.
 32. Gahr, Nina, Kassa Darge, Gabriele Hahn and Björn W Kreher, et al. "Diffusion-Weighted MRI for Differentiation of Neuroblastoma and Ganglioneuroblastoma/Ganglioneuroma." *Eur J Radiol* 79(2011): 443-446.
 33. Neubauer, Henning, Mengxia Li, Verena Rabea Mueller and Thomas Pabst, et al. "Diagnostic Value of Diffusion-Weighted MRI for Tumor Characterization, Differentiation and Monitoring in Pediatric Patients with Neuroblastic Tumors." *Röfo-Fortschritte Auf Dem Gebiet Der Röntgenstrahlen Und Der Bildgebenden Verfahren* 189(2018): 640-650.
 34. Serin, Halil Ibrahim, Sureyya Burcu Gorkem, Selim Doganay and Saliha Cıracı, et al. "Diffusion Weighted Imaging In Differentiating Malignant And Benign Neuroblastic Tumors." *Jpn J Radiol* 34(2016): 620-624.
 35. Demir, Senay, Naime Altinkaya, Nazim Emrah Kocer and Ayse Erbay, et al. "Variations in Apparent Diffusion Coefficient Values Following Chemotherapy in Pediatric Neuroblastoma." *Diagn Interv Radiol* 21(2015): 184.
 36. Jacobs, Filip, Hubert Thierens, A Piepsz and Klaus Bacher, et al. "Optimised Tracer-Dependent Dosage Cards to Obtain Weight-Independent Effective Doses." *Eur J Nucl Med Mol Imaging* 32(2005): 581-588.
 37. Linet, Martha S, Kwang Pyo Kim and Preetha Rajaraman. "Children's Exposure to Diagnostic Medical Radiation and Cancer Risk: Epidemiologic and Dosimetric Considerations." *Paediatr Radiol* 39(2009): 4-26.
 38. Laverdière, Caroline, Qi Liu, Yutaka Yasui and Paul C Nathan, et al. "Long-Term Outcomes in Survivors of Neuroblastoma: A Report from the Childhood Cancer Survivor Study." *J Natl Cancer Inst* 101(2009): 1131-1140.
 39. Mostoufi-Moab, Sogol, Kristy Seidel, Wendy M Leisenring and Gregory T Armstrong, et al. "Endocrine Abnormalities in Aging Survivors of Childhood Cancer: A Report from the Childhood Cancer Survivor Study." *J Clin Oncol* 34(2016): 3240.
 40. Chemaitilly, Wassim, Laurie E Cohen, Sogol Mostoufi-Moab and Briana C Patterson, et al. "Endocrine Late Effects in Childhood Cancer Survivors." *J Clin Oncol* 36(2018): 2153-2159.
 41. Müller, Lil-Sofie Ording, Derk Avenarius and Øystein E Olsen. "High Signal in Bone Marrow at Diffusion-Weighted Imaging with Body Background Suppression (DWBS) in Healthy Children." *Pediatr Radiol* 41(2011): 221-226.
 42. Kwee TC, Takahara T, Ochiai R and Niewelstein RA, et al. Diffusion-Weighted Whole-Body Imaging with Background Body Signal Suppression (DWBS): Features and Potential Applications in Oncology. *Eur Radiol* 9(2008): 1937-1952.
 43. Petralia, Giuseppe, Anwar R Padhani, Paola Pricolo and Fabio Zugni, et al. "Whole-Body Magnetic Resonance Imaging (WB-MRI) In Oncology: Recommendations and Key Uses." *Radiol Med* 124(2019): 218-233.
 44. Petralia, Giuseppe and Anwar R Padhani. "Whole-Body Magnetic Resonance Imaging in Oncology: Uses and Indications." *Magn Reson Imaging Clin N Am* 26(2018): 495-507.

How to cite this article: Olianti, Catia, Perrone A, Michela Allocca and Marco Di Maurizio, et al. "Whole-Body MRI and Whole Body [123I]-I-mIBG Scintigraphy: A Comparison in Intermediate and High Risk Neuroblastoma and validation of SIOPEN Scoring System in WB-MRI." *J Mol Genet Med* 15(2021): 505.